

# Demineralization Inhibition by High-Speed Scanning of 9.3 $\mu\text{m}$ CO<sub>2</sub> Single Laser Pulses Over Enamel

Ali H. Badreddine,<sup>1\*</sup> Stephen Couitt,<sup>1</sup> Julia Donovan,<sup>1</sup> Roni Cantor-Balan,<sup>1</sup> Charles Kerbage,<sup>1</sup> and Peter Rechmann<sup>2</sup>

<sup>1</sup>Convergent Dental, Inc., 140 Kendrick St Bldg C3, Needham, Massachusetts 02494

<sup>2</sup>Department of Preventive and Restorative Dental Sciences, School of Dentistry, University of California at San Francisco, 707 Parnassus Avenue, San Francisco, California 94143

**Background and Objective:** In vitro studies were conducted to evaluate the use of an automated system for high-speed scanning of single 9.3  $\mu\text{m}$  CO<sub>2</sub> laser pulses in the inhibition of caries-like lesion formation in the enamel of extracted human molars. The effect of the laser in generating an acid-resistant layer and the effect of the layer on inhibiting surface mineral loss during pH cycling was explored. **Study Design/Materials and Methods:** Laser irradiation was performed with fluences of 0.6, 0.8, and 1.0 J/cm<sup>2</sup> for single pulses of 1 mm diameter (1/e<sup>2</sup>), with pulse durations of 17, 22, and 27 microseconds, respectively. The laser was scanned at a 750 Hz pulse repetition rate in an automated pattern covering an area of 7 mm<sup>2</sup> in 0.3 sec. Six treatment groups were investigated: three groups for each fluence for laser-only and three for laser irradiation with additional fluoride from a toothpaste slurry (sodium fluoride at 1100 ppm). Each group used non-irradiated areas, which included untreated controls for the laser-only groups and a fluoride-only treatment for the groups with additional fluoride. pH cycling was performed on both groups, followed by microhardness testing to determine the relative mineral loss ( $\Delta Z$ ) from a caries-like formation and surface mineral loss ( $\Delta S$ ).

**Results:** Laser irradiation with the 9.3  $\mu\text{m}$  CO<sub>2</sub> laser generated an acid-resistant layer of about 15  $\mu\text{m}$  in depth. For the laser-irradiated samples with additional fluoride application, the relative mineral loss ( $\Delta Z$ ) was 113  $\pm$  63 vol% $\cdot\mu\text{m}$ , while for those with only fluoride application  $\Delta Z$  was 572  $\pm$  172 vol% $\cdot\mu\text{m}$ . At the highest fluence (1.0 J/cm<sup>2</sup>) used, an 80.2% inhibition of caries-like lesion was measured by  $\Delta Z$ . Using only laser irradiation at the highest fluence resulted in an inhibition of caries-like lesion of 79.5% for the irradiated samples ( $\Delta Z = 374 \pm 149$  vol% $\cdot\mu\text{m}$ ) relative to the control ( $\Delta Z = 1826 \pm 325$  vol% $\cdot\mu\text{m}$ ). Surface microhardness tests resulted in an inhibition of surface softening, as measured by the Knoop Hardness Value (KHN) (108  $\pm$  33 KHN for laser irradiated with additional fluoride, for non-irradiated controls with fluoride only 52  $\pm$  16 KHN). Inhibition of surface loss was observed for all laser fluences, but the maximum surface loss for the untreated control group was only 2.2  $\pm$  0.49  $\mu\text{m}$ .

**Conclusions:** The results demonstrate a significant benefit of the 9.3  $\mu\text{m}$  CO<sub>2</sub> laser at fluences of 0.6, 0.8, and

1.0 J/cm<sup>2</sup> in caries-like lesion inhibition as measured by the relative mineral loss in depth and surface mineral loss, without significant damage to the enamel. Additionally, inhibition of surface softening and surface loss during pH cycling was observed. The surface loss was small compared with the overall lesion depth and thickness of the generated acid-resistant layer. *Lasers Surg. Med.* © 2020 Wiley Periodicals LLC

**Key words:** 9.3  $\mu\text{m}$  CO<sub>2</sub> laser; erosion; caries; human enamel; fluoride uptake; microhardness; demineralization; remineralization; pH cycling

## INTRODUCTION

In caries prevention, acid resistance studies on tooth enamel have focused on the use of fluoride to form fluorapatite [1,2], or on using laser irradiation to induce structural changes of the surface or remove acid-soluble impurities such as carbonate groups [2–5]. The removal of carbonate groups from enamel, which has been explored since the 1970s [6–13], is achieved when enamel reaches a temperature of at least 400°C, at which point carbonate begins to outgas as CO<sub>2</sub>. Lasers such as Er:YAG and Nd:YAG, with enamel absorption coefficients of ~800 and <1 cm<sup>-1</sup>, respectively, are absorbed primarily by hydroxyl groups in water and hydroxyapatite and have been demonstrated to have some success in preventing caries formation [5,6,14,15]. CO<sub>2</sub> lasers, particularly those at 9.3 and 9.6  $\mu\text{m}$  wavelengths, are highly absorbed by phosphate groups in the enamel, with absorption coefficients of 5500 and 8000 cm<sup>-1</sup>, respectively [5,16–21], and therefore are capable of rapidly raising the tissue temperature to a degree at which carbonate is removed. Subsequently,

Conflict of Interest Disclosures: All authors have completed and submitted the ICMJE Form for Disclosure of Potential Conflicts of Interest and none were reported.

\*Correspondence to: Ali H. Badreddine, Convergent Dental, Inc., 140 Kendrick St. Bldg C3 Needham, MA 02494. E-mail: abadreddine@convergentdental.com

Accepted 12 October 2020

Published online 00 Month 2020 in Wiley Online Library (wileyonlinelibrary.com). DOI 10.1002/lsm.23340

irradiation with these CO<sub>2</sub> lasers can increase acid resistance with minimal undesired damage [7,8,22,23].

There is sufficient evidence to support the use of short-pulsed laser irradiation at 9.3 and 9.6  $\mu\text{m}$  to change the composition of surface enamel and make it more resistant to the formation of carious lesions [23]. Rechmann et al. [8] performed a controlled, randomized, single-blinded clinical trial irradiating fissures of second molars with a short-pulsed 9.6  $\mu\text{m}$  CO<sub>2</sub> laser. The irradiation combined with fluoride varnish application significantly inhibited carious lesions in human mouths during an observation period of one year. More recently, Rechmann et al. [24] showed in an *in vitro* study that a scanning beam enables caries resistance without apparent enamel melting.

The goal of this study was to evaluate the effectiveness of 9.3  $\mu\text{m}$  CO<sub>2</sub> laser irradiation to reduce dental enamel mineral loss and to inhibit a caries-like lesion formation with automated scanning of single-pulse irradiation at a high repetition rate over an area of about 7 mm<sup>2</sup>. The energy delivery method was designed to allow for a clinically relevant application in terms of treatment speed and safe energy levels not resulting in significant surface damage or overheating of the pulp. In addition, the effects of laser irradiation on enamel were investigated through a characterization of the acid-resistant layer and measurement of surface mineral loss both with and without the use of additional fluoride.

## MATERIALS AND METHODS

### Laser Settings

A 9.3  $\mu\text{m}$  CO<sub>2</sub> laser (Solea, Convergent Dental, Inc., Needham, MA) was used with the irradiation parameters described in Table 1. The native beam diameter was modified to 1 mm (measured by  $1/e^2$  method) and collimated at the output of the handpiece. The native beam was scanned over the irradiated surface at a pulse scan rate of 750 Hz using a pair of computer-controlled mirrors in a pattern creating a uniform spacing of 0.2 mm between centers of each adjacent single laser spot. This distribution of single irradiation spots was developed to decrease the overall treatment time and to distribute the accumulation of heat energy from irradiation over a larger area to prevent an unacceptable increase in pulp temperature. To assist in cooling, a regulated delivery system with airflow through the handpiece was used while irradiating with the laser [5,25]. Laser fluence was varied by changing the pulse duration to 17, 22, and 27 microseconds to achieve fluences of 0.6, 0.8, and 1.0 J/cm<sup>2</sup>, respectively. The distance from the tip of the handpiece output to the sample surface was maintained at a set position of 10 mm to further ensure uniform delivery of laser energy and airflow on the surface enamel.

### Test Samples for Assessment of Acid-Resistant Layer

Five sound human enamel samples mounted in acrylic resin and polished to 1  $\mu\text{m}$  diamond suspension grit finish (Therametrics, Inc., Indianapolis, IN) were used for the

investigation of the formation and properties of the acid-resistant layer. The samples had been exposed to 0.1% thymol solution during shipment and were less than 3 months old after extraction.

To investigate the acid-resistant layer created by laser irradiation, the mounted samples were serially polished up to 6  $\mu\text{m}$  diamond suspension grit from the side to expose a cross-section of both the laser-irradiated and non-irradiated areas. The original surface that had been laser-irradiated was masked with an acid-resistant tape (3M, Maplewood, MN). The cross-section surface was exposed to five drops of hydrochloric acid (1 M HCl) for 1 minute to erode the underlying non-irradiated enamel and expose the acid-resistant layer, then rinsed thoroughly with distilled water.

### Microscopy Images

The blocks were imaged under a 3D digital reflection Hirox RH-2000 microscope (Hirox-US, Hackensack, NJ) with and without cross-polarization illumination to capture the surface characteristics. 3D image stacks were obtained at 1000 $\times$  magnification using the integrated built-in stepping motor with 0.8  $\mu\text{m}$  steps in the z-axis. The range was manually selected to ensure all pixels were in focus at the same position in the range. This was done to ensure that the curvature of the surface could be corrected for, and the images show a two-dimensional (2D) projection of the 3D curved surface. To measure the acid-resistant layer, the cross-section of a sample was imaged at 2000 $\times$  magnification and a 0.5  $\mu\text{m}$  step size.

### Test Samples Preparation

Seventy-four human molars with no signs of caries or fluorosis and less than 3 months after extraction were obtained and stored in thymol solution. The molars were mounted in 1" acrylic cylinders with the full crown exposed (all sides and occlusal surface) (Therametrics, Inc.). The molar samples were sonicated for 5 minutes in distilled water. The samples were then air dried and split into six groups. Samples of group 1–3 underwent pH cycling without additional fluoride and samples of group 4–6 with additional fluoride. The fluoride used was a sodium-fluoride-toothpaste slurry mixed for 1 min, applied after each step in the cycling, using a 1:3 ratio of 1100 ppm F

**TABLE 1. Laser Irradiation Parameters**

Parameter	Value		
Beam diameter (mm)	1.0		
Beam divergence	Collimated		
Pulse durations ( $\mu\text{s}$ )	17	22	27
Fluence (J/cm <sup>2</sup> )	0.6	0.8	1.0
Average power (W)	3.5	4.6	5.7
Peak power (W)	290		
Pulse repetition rate (Hz)	750		
Pattern area (mm <sup>2</sup> )	7		
Distance from the tip of the handpiece to sample surface (cm)	1.0		

toothpaste (Crest cavity protection; Procter and Gamble, Inc., Cincinnati, OH) to distilled water. Samples of groups 1 and 4 were laser-irradiated at a fluence of  $0.6 \text{ J/cm}^2$ , of groups 2 and 5 at  $0.8 \text{ J/cm}^2$ , and of groups 3 and 6 at  $1.0 \text{ J/cm}^2$  on either side of an area with the least curvature of the buccal or lingual side of the crown as shown in Figure 1. A non-irradiated control area was maintained between the laser-irradiated areas. An acid-resistant, quick curing nail polish was used to mask the boundaries between laser-irradiated and non-irradiated regions along the entire height of the molar from the mounted base to the occlusal surface. Some loss of samples occurred due to polishing damage or other immeasurability of the sample.

### pH Cycling

Demineralization solution was made in the form of a 75 mM acetate buffer with 2 mM calcium and phosphate, pH balanced to 4.4 using NaOH or HCl where needed. Remineralization solution was made from 0.1 M Tris, 0.8 mM calcium, and 2.4 mM phosphate, pH balanced to 7.1. A 9-day pH cycling regimen with the aforementioned solutions was followed as described by Rechmann et al. [23,26,27], with steps of 6 hours in demineralization and 18 hours in remineralization. Half the samples were exposed to the fluoride-toothpaste slurry for 1 minute after each step in the cycling. After five cycles, the solutions were replaced with fresh solutions from the same batch. After cycling, the samples were stored in distilled water for no more than two weeks until the measurements were performed.

### Cross-Sectional Microhardness Measurements

To determine the relative mineral loss  $\Delta Z$  under the laser-treated area, a cross-section perpendicular to the laser-irradiated surface area was created by polishing the blocks from the occlusal surface to the approximate middle of the treated areas. Up to six samples at a time were polished using an automated polisher, Metkon Forcipol 1v (Kemet International, Kent, ME), with a 600-grit polishing pad until a flat cross-section in the laser-irradiated areas was reached. Then, the samples were individually hand-polished with a  $1 \mu\text{m}$  diamond suspension to remove polishing marks for the cross-sectional microhardness testing.

The samples were serially indented using a microhardness indenter Matsuzawa Seiki DMH-2, (Matsuzawa, Akita Pref, Japan) in a straight line under the surface with 25 g loads for a duration of 10 seconds for each indent with steps of  $15 \mu\text{m}$  starting at  $15 \mu\text{m}$  from the outer surface until a depth of  $200 \mu\text{m}$  was reached. The length of each indent was measured as the long diagonal generated from the Knoop tip using the digital microscope (Hirox RH-2000) at  $2000\times$  magnification. The volume percent mineral content was then calculated at each indentation position using the formula  $\text{vol}\% = 4.3\sqrt{\text{KHN}} + 11.3$ , where KHN is the Knoop Hardness Values obtained from the length of the indents [27,28].  $\Delta Z$ , a measure of depth mineral loss, was then calculated as the area under the curve according to Stookey et al. [27].

### Surface Microhardness Measurements

After  $\Delta Z$  was determined, each sample was turned on its side so that the laser-irradiated and control areas were facing up. Samples were then polished on this same side

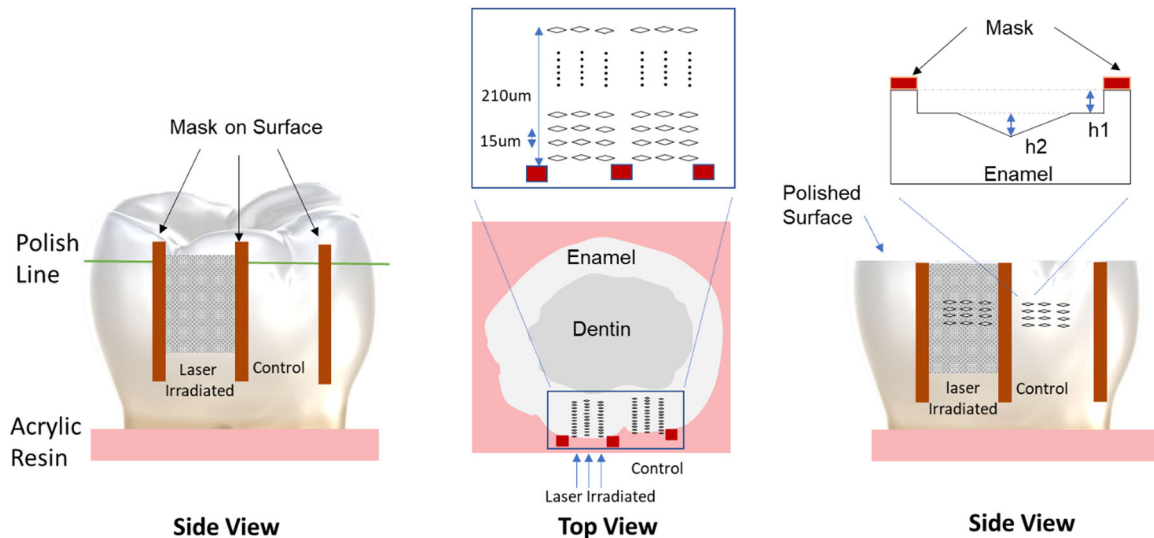


Fig. 1. (Left) Side-view depiction of a human molar in an acrylic resin mount with a laser-irradiated and non-irradiated control separated by masked regions over the outer surface of the exposed tooth and location of the transverse cross-section from polishing. (Middle) Top-view depiction of serial indentations to obtain relative mineral loss after the sample being polished. The indents were made  $15 \mu\text{m}$  apart under the surface to a depth of  $210 \mu\text{m}$ . (Right) Side-view of surface indentations made to obtain the surface mineral loss.  $h_1$  and  $h_2$  are the surface loss height and indent height, respectively. These are used to calculate  $\Delta S$  to represent the overall surface mineral loss.

until half of the sample had been removed. Occasional loss of samples occurred due to unexpected damage to the surface or mishandling during polishing. Using the same indenter, samples were indented at a total of 10 different locations for each region of each sample, on both the laser-irradiated and non-irradiated control surfaces. The symmetry and quality of each indent was checked under the microscope and the lengths of the indents were measured.

The surface loss was measured at the edge of the nail polish using the built-in 3D controller with submicron accuracy on the microscope. The surface height was determined as the change in height from the edge of the masked surface to the top of the adjacent unmasked enamel surface. Measurements were taken along the entire length of every boundary region every 50  $\mu\text{m}$ , obtaining 10 measurements for each boundary region.

While  $\Delta Z$  is a measure of the volumetric mineral loss associated with a caries-like formation under the surface,  $\Delta S$  was calculated to capture the overall demineralization effect on the surface mineral loss. This measure includes the surface hardness and surface loss simultaneously. The surface loss component of  $\Delta S$  is treated as mineral volume removed (85% max mineral content on average) multiplied by the measured surface loss ( $h1$ ), as depicted in Figure 1. The height of each indent ( $h2$ ) is calculated by taking the length measurement and the known geometry of a Knoop tip. The vol% mineral remaining on the surface structure was calculated in a method identical to that of  $\Delta Z$  (above). The two values were combined by the formula  $\Delta S = [h1 \times 85\% + h2 \times (85\% - \text{vol}\%)]$ .

### Statistical Methods and Sample Size Calculation

A pilot study had been performed to determine the mean  $\Delta Z$  for the groups. We calculated that for an  $\alpha$  of 0.05 and a power of 80%, a minimum of 10, 10, and 5 samples for the 0.6, 0.8, and 1.0 J/cm<sup>2</sup>, respectively, was needed. For this study, group 1 used 14 samples, group 2 used 15 samples, group 3 used 8 samples, group 4 used 14 samples, group 5 used 15 samples, and group 6 used 8 samples, with the expectation of some loss of samples. The number of samples for groups with similar mean  $\Delta Z$  values were similar to those of previous work [23].

Data were analyzed in Minitab 18 (Minitab, Inc. State College, PA) on a log scale using Welch's analysis of variance (ANOVA) and post-hoc Games-Howell tests for comparison of individual groups. These tests were selected to minimize the effects of differences in group sample size or variance on the statistical results.

### Pulpal Temperature

Following the previous work [29,30], type J thermocouples (5TC-TT-J-36-36; Omega Engineering, Norwalk, CT) were placed through a drilled hole through the root into the roof of the pulp chamber of 7 extracted teeth with thermally conductive paste and tape (3M). X-ray images of the teeth were acquired to confirm that the thermocouple tip was mounted correctly, touching the pulp chamber ceiling. The tooth was held upright in clay on a heating plate and its baseline temperature was maintained at  $35.0 \pm 2.0^\circ\text{C}$ . The change in

temperature was recorded during 40 seconds of continuous irradiation over the tooth surfaces, with the same settings as described above at the highest fluence used in this study (1 J/cm<sup>2</sup>). Data were collected using a temperature logger (HH806U; Omega Engineering). The duration of irradiation was equivalent to the time sufficient to treat a single tooth, as a single delivery of the scanned pattern covers 7 mm<sup>2</sup> in 0.3 seconds. A time delay of 0.8 seconds after each delivery of the scanned pattern was used to mimic the time needed for a healthcare worker to move target locations on the tooth in a clinical setting. The largest tooth surface averages around 284 mm<sup>2</sup> according to Cohen [31]; thus at total of 12 seconds of irradiation would cover the whole tooth surface.

## RESULTS

Figures 2 and 3 are the regular and cross-polarized images, respectively, representative of the three fluence levels for the non-irradiated and irradiated samples. Each of the cross-polarized images is at identical locations to the corresponding regular surface images. The regular images reveal minor superficial changes from laser irradiation, with some small amount of melting observed at 1 J/cm<sup>2</sup> in the "hottest" spots. The crazing of the surface caused by laser irradiation at the fluences used in this study is evident but difficult to distinguish under regular microscopic imaging. However, crazing from irradiation is obvious in the cross-polarized images since it occurs several microns into the structure. Additionally, individual enamel rods can be seen under the crazed surface for areas treated with 0.6 and 0.8 J/cm<sup>2</sup>. These rods are harder to distinguish under the areas treated with 1 J/cm<sup>2</sup>.

### Acid-Resistant Layer

Figure 4A is a cross-section image of enamel exposed to hydrochloric acid for one minute, as described in the methods and materials section above. An acid-resistant layer in the range of 15  $\mu\text{m}$  depth was created by the laser irradiation at a fluence of 0.8 J/cm<sup>2</sup>. This acid-resistant layer is exhibited as an undissolved protrusion above the underlying enamel that had experienced a rapid dissolution to the HCl (as expected) and is out of focus in the microscope image. Figure 4B shows a cross-section of the enamel for a non-irradiated area that dissolved uniformly with no acid-resistant layer observed. Figure 4C and D are 3D image stacks of the enamel samples that reveal the acid-resistant layer as an area near the surface not eroded away by the HCl for the laser-irradiated sample and a flat, evenly eroded away area for the non-irradiated sample.

### Pulpal Temperature

Thirty seconds of laser irradiation on the surfaces of the extracted teeth resulted in an average temperature increase of  $2.2^\circ\text{C} \pm 1.1$  in the pulp chamber. This increase is considered as safe for the pulpal tissue [32–34].

### Relative Mineral Loss $\Delta Z$

$\Delta Z$  values, shown in Table 2 and Figure 5A, provide a measure of caries-like lesion formation [7,28] and serve as

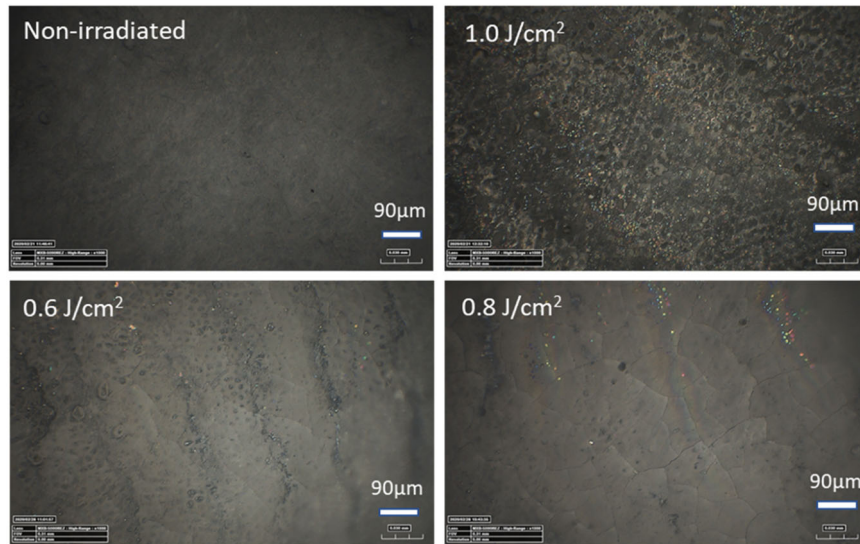


Fig. 2. Microscope images of non-irradiated and irradiated samples for three fluences at 1000 $\times$  magnification. There was minimal surface damage or structural modifications from laser irradiation. At the highest fluence used, some early signs of melting were observed in the “hottest” areas of irradiation.

a metric for comparing treatments with different laser settings. For the range of fluences used, there were no visually observed superficial structural changes, except for signs of very minor crazing under the surface, particularly for the areas irradiated with 1.0 J/cm<sup>2</sup>.

Welch's ANOVA revealed that significant differences in  $\Delta Z$  occurred between the treatment groups ( $F_{11,40} = 81.0$ ,  $P < 0.001$ ). The average reduction in  $\Delta Z$  from the use of fluoride alone (groups 4–6) without laser irradiation was 65% ( $P < 0.001$ ). Reductions in  $\Delta Z$  from laser irradiation alone were observed, too (see groups 1–3 in Table 2), indicating that

effective remineralization occurs with or without the presence of additional fluoride. Post-hoc Games–Howell tests showed that the combination treatment of laser irradiation and additional fluoride provided the most significant benefit in reducing  $\Delta Z$  for each of the laser fluences used ( $P < 0.01$  for all). Although pH cycling with additional fluoride alone revealed a significant benefit in caries inhibition, application of fluoride to the pH cycling after laser irradiation resulted in the most significant reduction in mineral loss, with as high as 92% ( $P = 0.001$ ) reduction in  $\Delta Z$  compared with the untreated control areas.

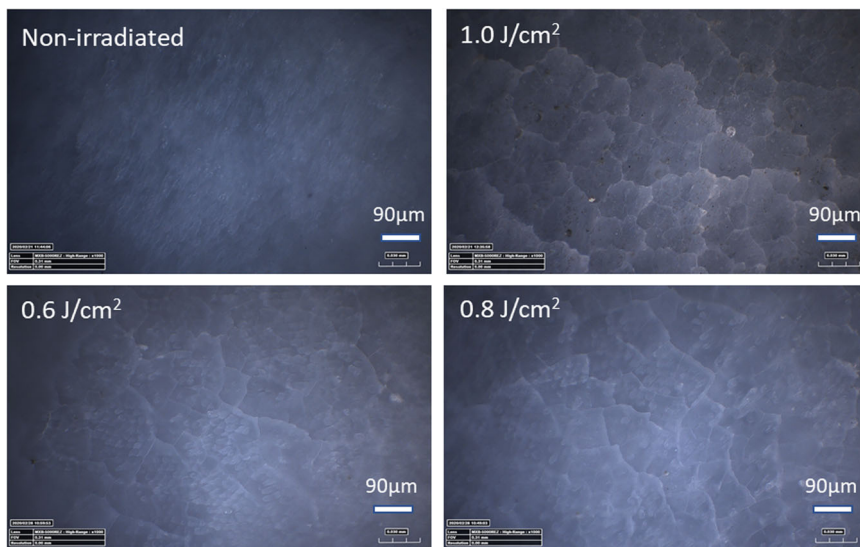


Fig. 3. Cross-polarized microscope images of non-irradiated and irradiated teeth for three fluences at 1000 $\times$  magnification. Crazing of the surface from laser irradiation is evident at all three fluences. Individual enamel rods are also evident in all images.

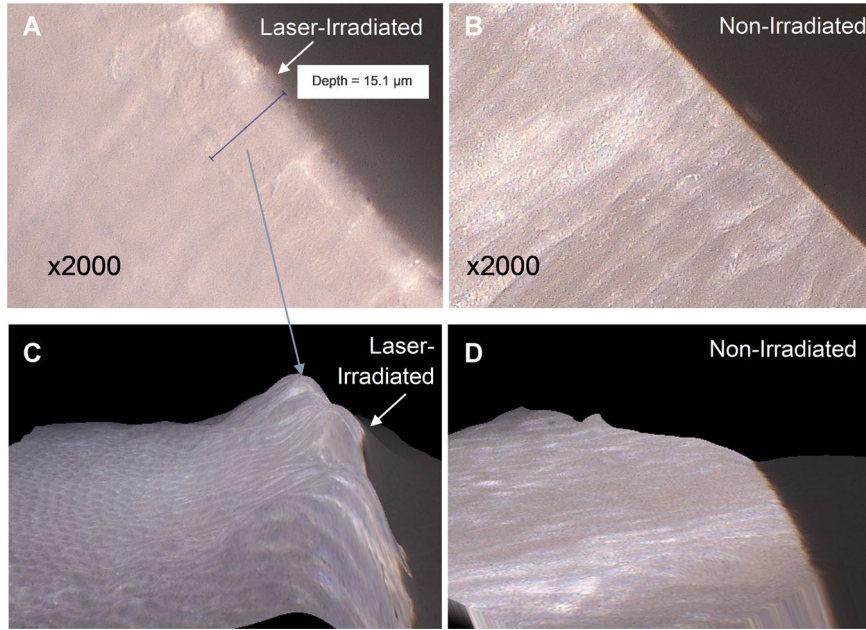


Fig. 4. (A) Cross-section image of dental enamel showing an acid-resistant layer of 15  $\mu\text{m}$  in thickness generated by the 9.3  $\mu\text{m}$  CO<sub>2</sub> laser at a fluence of 0.8 J/cm<sup>2</sup> not eroded away by 1 minute HCl acid erosion. (B) Cross-sectional image of a non-irradiated dental enamel sample showed uniform dissolution and no resistance to mineral dissolution after 1-minute exposure to HCl. (C) A three-dimensional (3D) image stack of the cross-sectioned enamel under a laser-irradiated area is shown, revealing the acid-resistant layer. (D) A 3D image stack of a section under the non-irradiated area reveals a relatively uniform etching due to the HCl acid solution.

### Surface Mineral Loss $\Delta S$

Figure 5C and D show the surface loss and microhardness measurements, and Figure 5B shows their combination, in the form of  $\Delta S$ . Welch's ANOVA applied to  $\Delta S$  values showed that there were significant differences between groups ( $F_{11,36} = 29.7$ ,  $P < 0.001$ ). The general trends for  $\Delta S$  were similar to those observed for  $\Delta Z$  in relation to laser fluence.  $\Delta S$  revealed that 9.3  $\mu\text{m}$  laser irradiation alone inhibited surface mineral loss by as much as ~68% ( $P = 0.009$ ). Furthermore, a combination of 1 J/cm<sup>2</sup> laser irradiation coupled with additional fluoride application from toothpaste showed a reduction in surface mineral loss of ~73% ( $P = 0.002$ ) compared with the non-irradiated control. The use of fluoride application without laser irradiation reduced surface mineral loss, but laser

irradiation had a much greater impact on inhibition of surface mineral loss (Table 3).

Figure 6 shows linear regression fits (on a log scale); data are averaged according to the treatment group. The treatment groups include a group for untreated controls, a group for samples only treated with fluoride, three groups for samples only irradiated with the laser at each of the fluences, and three groups for samples treated with fluoride and laser irradiation. Both sets of values for  $\Delta Z$  and  $\Delta S$  followed a log-normal distribution. The linear fits for these two sets have similar slopes, 1.1 ( $R^2 = 0.95$ ) for additional fluoride, and 1.3 ( $R^2 = 0.96$ ) for no additional fluoride. The overall effect of fluoride on caries and acid resistance can be quantified by the vertical and horizontal shifts in the curve, revealing that fluoride provides a

TABLE 2. Relative Mineral Loss Data

Group	Additional fluoride	Laser fluence (J/cm <sup>2</sup> )	Laser		No laser		Laser reduction, % $\Delta Z$	$P$ value (95%)
			$\Delta Z$ (std)	$\Delta Z$ (n)	$\Delta Z$ (std)	$\Delta Z$ (n)		
1	No	0.6	1025 (253) <sup>a</sup>	13	1610 (247) <sup>e</sup>	13	36.3	0.001
2	No	0.8	763 (322) <sup>ab</sup>	15	1809 (498) <sup>e</sup>	15	57.8	<0.001
3	No	1.0	374 (149) <sup>bcd</sup>	5	1826 (325) <sup>e</sup>	7	79.5	0.002
4	Yes	0.6	349 (54.1) <sup>cd</sup>	12	591 (103) <sup>b</sup>	12	40.9	<0.001
5	Yes	0.8	216 (145) <sup>d</sup>	13	665 (176) <sup>b</sup>	13	67.5	<0.001
6	Yes	1.0	113 (62.9) <sup>d</sup>	7	572 (172) <sup>bc</sup>	8	80.2	0.01

Groups that share a lower-case letter are not significantly different.

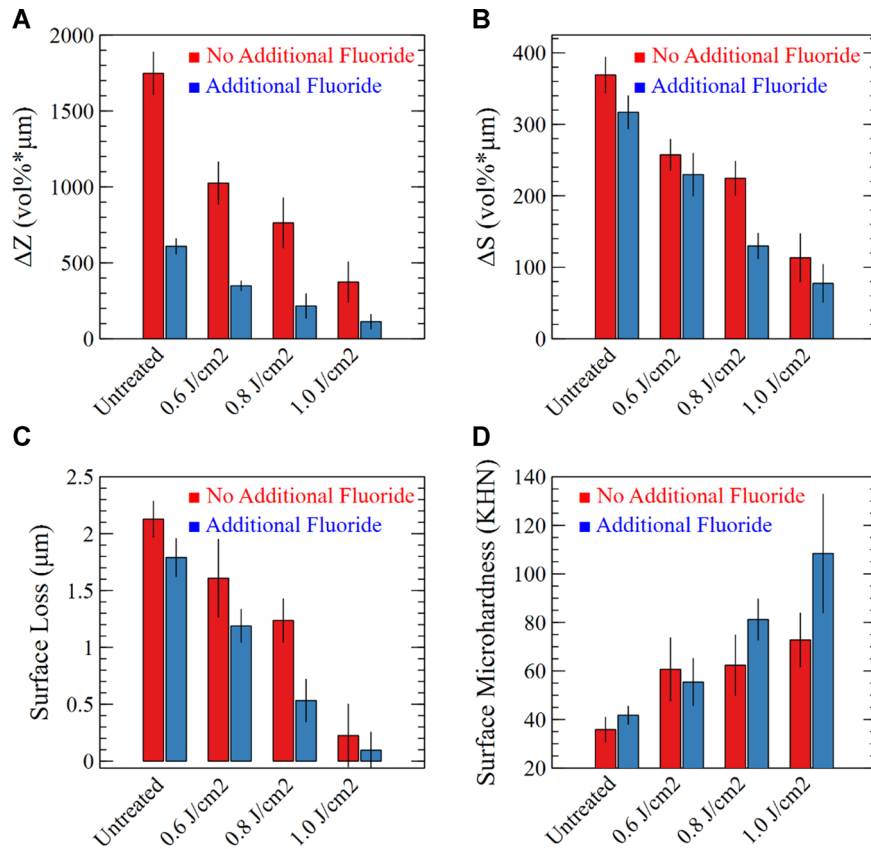


Fig. 5. (A) Volume percent mineral loss due to caries-like formation ( $\Delta Z$ ) demonstrated a significant benefit from additional fluoride alone. This benefit was also observed from laser irradiation without additional fluoride at all three fluence levels used. A combination of the two yielded the most significant reduction in  $\Delta Z$ , with up to 6 $\times$  less than the baseline both with and without fluoride. (B)  $\Delta S$  is a metric for combining surface loss (C) and surface microhardness (D) measurements, calculated in a manner similar to  $\Delta Z$ .  $\Delta S$  showed a similar trend as  $\Delta Z$  with increasing laser fluence, but revealed less significance in surface mineral loss resistance from use of additional fluoride compared with lasing.

40–50% inhibition in caries formation and surface mineral loss. Averaged both with and without additional fluoride, together  $\Delta Z$  and  $\Delta S$  were improved by ~36%, 56%, and 75% after laser irradiation of 0.6, 0.8, and 1.0 J/cm<sup>2</sup>, respectively, compared with areas without laser irradiation.

## DISCUSSION

Laser irradiation at 9.3  $\mu\text{m}$  wavelength creates a more acid-resistant form of hydroxyapatite happening at temperatures at which a significant amount of naturally occurring carbonate groups in the enamel are removed, consequently

**TABLE 3. Surface Mineral Loss Data**

Group	Additional fluoride	Laser fluence (J/cm <sup>2</sup> )	Laser		No laser		Laser reduction, % $\Delta S$	<i>P</i> value (95%)
			$\Delta S$ (std)	$\Delta S$ (n)	$\Delta S$ (std)	$\Delta S$ (n)		
1	No	0.6	257.5 (34.5) <sup>abc</sup>	10	387.6 (45.2) <sup>e</sup>	10	33.6	<0.001
2	No	0.8	224.6 (46.4) <sup>ab</sup>	15	364.7 (83.4) <sup>e</sup>	15	38.4	<0.001
3	No	1.0	113.4 (38.1) <sup>ad</sup>	5	355.3 (64.0) <sup>ce</sup>	5	68.1	0.009
4	Yes	0.6	229.7 (50.1) <sup>ab</sup>	11	335.1 (53.9) <sup>e</sup>	11	31.4	0.005
5	Yes	0.8	129.9 (32.1) <sup>d</sup>	13	327.9 (71.8) <sup>ce</sup>	13	60.3	<0.001
6	Yes	1.0	77.5 (35.2) <sup>d</sup>	7	287.7 (61.2) <sup>ace</sup>	7	73.1	0.002

Groups that share a lower-case letter are not significantly different.

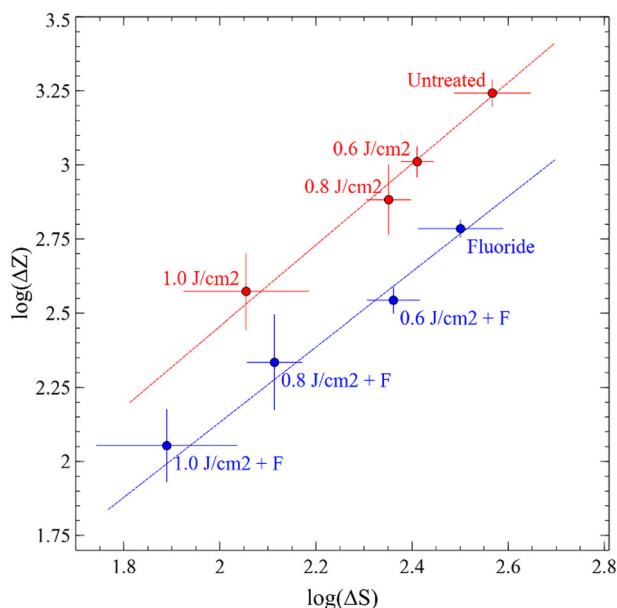


Fig. 6. Average of log-transformed  $\Delta Z$  and  $\Delta S$  values according to treatment groups is plotted with 95% confidence intervals and linear fits for the two groups (with and without additional fluoride). The linear regression fits have slopes of 1.1 ( $R^2 = 0.95$ ) for the group with additional fluoride and 1.3 ( $R^2 = 0.96$ ) for the one with no additional fluoride.

generating an acid-resistant layer [35]. Other organic components, which largely exist as a glue-like network holding adjacent rods together, are also removed or shrink near the surface during irradiation. Together, these surface changes have been described previously as a “crazing” of the surface [36]. The formation of fluoride-containing hydroxyapatite further reduces the solubility of the acid-resistant layer. The benefit of laser irradiation under laser conditions described in this study, with or without the use of additional fluoride, is significant. The presented results are in general agreement with findings reported previously for the  $\Delta Z$  relative mineral loss in depth [23] due to acid challenges. The study served as a verification that the computer-assisted scanning method of a single laser pulse over enamel surfaces at a high repetition rate will be effective for a clinical application.

Although this method is a high-speed scanning of laser irradiation, the temperature rise in the pulp was lower than the traditionally accepted 5.5°C temperature increase at which irreversible pulpal damage is thought to occur [32]. Further studies of this temperature rise in worst-case scenarios, such as teeth with eroded or hypomineralized enamel, or teeth that are small and have a relatively short distance to the pulp, may be necessary to ensure the safety of this laser energy delivery in a clinical setting. In such worst-case scenarios, a higher rise in temperature could possibly occur with the laser irradiation levels presented here, but more recent work has argued that a higher temperature rise may be acceptable, with one study showing that even a rise of up to 11.2°C may not irreversibly damage the pulp [33].

This study also demonstrated a novel method of measuring the thickness of the laser created acid-resistant layer. Further work can be done to better characterize the acid-resistant layer, particularly concerning its thickness as a function of laser fluence and any variations of this thickness over the treated area. Such a characterization could be aided by correlating thickness with a reduction in carbonate groups measured by spectroscopy methods such as Fourier-transform infrared spectroscopy [5,16,17].

Surface mineral loss ( $\Delta S$ ) and relative mineral loss ( $\Delta Z$ ) in depth were both slowed significantly by laser irradiation at all applied fluences, with the amount of inhibition scaled directly with the fluence. This strongly indicated that any potential negative effects of the crazing, appearing as possible “weakened” sites, are insignificant, probably due to a remineralization effect from dissolved calcium and phosphates with or without the presence of fluoride. Indeed, the benefit of laser-generated acid resistance outweighs the potential risks associated with the observed minor structural changes to the surface. Additional studies are needed to investigate the effects of heating on the crystallographic properties of the enamel surface in response to this type of irradiation pattern.

With the introduction of fluoride in the remineralization—demineralization cycling process, the acid-resistant properties of the layer were enhanced as measured by the relative mineral loss  $\Delta Z$ . This is in large part due to the inherent resistance of fluorapatite to acid dissolution [27,37]. The laser-treated area may encourage uptake of fluoride by the surface, together with calcium and phosphate, resulting in the observed beneficial effect pairing laser and fluoride treatments, as described previously [38,39]. Nonetheless, in this study, the use of fluoride only provided a less significant inhibition of surface mineral loss after pH cycling, compared with the measured inhibition from laser irradiation alone. An explanation for this could be the relatively small amount of mineral loss from the surface after pH cycling and the acid resistance of the acid-resistant layer, which is much thicker than any observed surface loss. This suggests that the laser-modified enamel may be more acid-resistant than ordinary fluorapatite created when added to the pH cycling. Further studies using energy-dispersive X-ray spectroscopy in conjunction with scanning electron microscopy could be performed to investigate the formation or precipitation of less soluble compounds such as globules of CaF<sub>2</sub> after pH cycling.

The present study also showed a direct log-linear correlation between the surface mineral loss ( $\Delta S$ ) and the  $\Delta Z$  mineral loss in a carious lesion. An explanation may be that complete remineralization back to the original mineral density may not be possible, as the mineral deposition is random and may introduce insufficiently packed crystals. For this reason, this observation may be confined to the method of pH cycling performed *in vitro*. Nonetheless, this surface metrics may serve as a simple method to estimate the total extent of demineralization occurring during a pH cycling or acid erosion protocol and not able to be determined by other existing single metrics or methods.

In a clinical application, the resistance to acid may be further enhanced by the use of high-concentration fluoride applications, such as prescription fluoride mouthwashes or varnishes, which would also help to quickly remineralize any weak sites with fluorapatite. As reported, the laser-irradiated areas and thus the crystals are capable of increasing the rate of fluoride uptake, and the effects have been demonstrated *in vivo* [8,39]. In this work, surface mineral loss and caries resistance were enhanced by around 50–60% using fluoride-containing toothpaste and can be increased by a further 40–80% using a 9.3  $\mu\text{m}$  CO<sub>2</sub> laser irradiation.

## CONCLUSION

A combination treatment of 9.3  $\mu\text{m}$  CO<sub>2</sub> laser irradiation and fluoride provides the strongest possible resistance to acid exposure and caries formation. In this study, acid resistance increased for all laser fluences tested, with 0.6, 0.8, and 1.0 J/cm<sup>2</sup>, using a scanning delivery mechanism of laser pulses with a beam diameter of 1 mm at a repetition rate of 750 Hz over a 7 mm<sup>2</sup> area. With a fluence of 1.0 J/cm<sup>2</sup> (corresponding to a pulse duration of 27 microseconds), in combination with sodium fluoride derived from a toothpaste, an 80.2% reduction in caries-like formation as well as a 73.1% reduction in surface mineral loss occurred. Any structural changes generated on the surface by laser irradiation were overcome by the remineralization of hydroxyapatite, particularly when assisted by fluoride. The reduction in caries formation and surface mineral loss is sixfold higher due to this treatment of a combination of fast CO<sub>2</sub> 9.3  $\mu\text{m}$  short-pulsed laser surface irradiation and additional fluoride application compared with just fluoride only and can be applied quickly and safely in a clinical setting.

## ACKNOWLEDGMENTS

Massachusetts Life Sciences provided funding for an internship involving part of this work. Convergent Dental, Inc. provided all funding for the experimental work.

## REFERENCES

- Zhu Y, Zhang X, Chen Y, et al. A comparative study on the dissolution and solubility of hydroxylapatite and fluorapatite at 25°C and 45°C. *Chem Geol* 2009;268(1-2):89–96. <https://doi.org/10.1016/j.chemgeo.2009.07.014>
- Shellis RP, Featherstone JDB, Lussi A. Understanding the chemistry of dental erosion. *Monogr Oral Sci* 2014;25:163–179. <https://doi.org/10.1159/000359943>
- Shi J, Klocke A, Zhang M, Bismayer U. Thermally-induced structural modification of dental enamel apatite: Decomposition and transformation of carbonate groups. *Eur J Mineral* 2005;17(5):769–775. <https://doi.org/10.1127/0935-1221/2005/0017-0769>
- Barinov SM, Rau JV, Cesaro SN, et al. Carbonate release from carbonated hydroxyapatite in the wide temperature range. *J Mater Sci Mater Med* 2006;17(7):597–604. <https://doi.org/10.1007/s10856-006-9221-y>
- Featherstone JDB, Fried D. Fundamental interactions of lasers with dental hard tissues. *Med Laser Appl* 2001;16(3):181–194. <https://doi.org/10.1078/1615-1615-00022>
- Kayano T, Ochiai S, Kiyono K, Yamamoto H, Nakajima S, Mochizuki T. Effects of Er:YAG laser irradiation on human extracted teeth. *J Stomatol Soc Japan* 1989;56(2):381–392. <https://doi.org/10.5357/koubyou.56.381>
- Rechmann P, Fried D, Le CQ, et al. Caries inhibition in vital teeth using 9.6- $\mu\text{m}$  CO<sub>2</sub>-laser irradiation. *J Biomed Opt* 2011;16(7):071405. <https://doi.org/10.1117/1.3564908>
- Rechmann P, Charland DA, Rechmann BMT, Le CQ, Featherstone JDB. In-vivo occlusal caries prevention by pulsed CO<sub>2</sub>-laser and fluoride varnish treatment—A clinical pilot study. *Lasers Surg. Med.* 2013;45(5):302–310. <https://doi.org/10.1002/lsm.22141>
- González-Rodríguez A, de Dios López-González J, del Castillo J, de DL, Villalba-Moreno J. Comparison of effects of diode laser and CO<sub>2</sub> laser on human teeth and their usefulness in topical fluoridation. *Lasers Med Sci* 2011;26(3):317–324. <https://doi.org/10.1007/s10103-010-0784-y>
- Cohen J, Featherstone JDB, Le CQ, Steinberg D, Feuerstein O. Effects of CO<sub>2</sub> laser irradiation on tooth enamel coated with biofilm. *Lasers Surg Med* 2014;46(3):216–223. <https://doi.org/10.1002/lsm.22218>
- Stern RH, Vahl J, Sognnaes RF. Lased enamel: Ultrastructural observations of pulsed carbon dioxide laser effects. *J Dent Res* 1972;51(2):455–460. <https://doi.org/10.1177/00220345720510023501>
- Beeking PO, Herrmann C, Zuhrt R. Examination of laser-treated tooth surfaces after exposure to acid. *Dtsch Stomatol* 1990;40(12):490–492.
- Steiner-Oliveira C, Nobre-dos-Santos M, Zero DT, Eckert G, Hara AT. Effect of a pulsed CO<sub>2</sub> laser and fluoride on the prevention of enamel and dentine erosion. *Arch Oral Biol* 2010;55(2):127–133. <https://doi.org/10.1016/j.archoralbio.2009.11.010>
- Ana PA, Bachmann L, Zezell DM. Lasers effects on enamel for caries prevention. *Laser Phys* 2006;16(5):865–875. <https://doi.org/10.1134/S1054660X06050197>
- Hossain M, Nakamura Y, Kimura Y, Yamada Y, Ito M, Matsumoto K. Caries-preventive effect of Er:YAG laser irradiation with or without water mist. *J Clin Laser Med Surg* 2000;18(2):61–65. <https://doi.org/10.1089/clm.2000.18.61>
- Corrêa-Afonso AM, Bachmann L, De Almeida CG, Corona SAM, Borsatto MC. FTIR and SEM analysis of CO<sub>2</sub> laser irradiated human enamel. *Arch Oral Biol* 2012;57(9):1153–1158. <https://doi.org/10.1016/j.archoralbio.2012.02.004>
- Zezell DM, Benetti C, Veloso MN, Castro PAA, Ana PA. FTIR spectroscopy revealing the effects of laser and ionizing radiation on biological hard tissues. *J Braz Chem Soc* 2015;26(12):2571–2582. <https://doi.org/10.5935/0103-5053.20150246>
- Nelson DGA, Wefel JS, Jongebloed WL, Featherstone JDB. Morphology, histology and crystallography of human dental enamel treated with pulsed low-energy infrared laser radiation. *Caries Res* 1987;21(5):411–426. <https://doi.org/10.1159/000261047>
- Featherstone JDB. The science and practice of caries prevention. *J Am Dent Assoc* 2000;131(7):887–899. <https://doi.org/10.14219/jada.archive.2000.0307>
- Featherstone JDB, Barrett-Vespone NA, Fried D, Kantorowitz Z, Seka W. CO<sub>2</sub> laser inhibition of artificial caries-like lesion progression in dental enamel. *J Dent Res* 1998;77(6):1397–1403. <https://doi.org/10.1177/00220345980770060401>
- Chan KH, Fried D. Selective ablation of dental caries using coaxial CO<sub>2</sub> (9.3- $\mu\text{m}$ ) and near-IR (1880-nm) lasers. *Lasers Surg Med* 2019;51(2):176–184. <https://doi.org/10.1002/lsm.23002>
- Esteves-Oliveira M, Pasaporti C, Heussen N, Eduardo CP, Lampert F, Apel C. Rehardening of acid-softened enamel and prevention of enamel softening through CO<sub>2</sub> laser irradiation. *J Dent* 2011;39(6):414–421. <https://doi.org/10.1016/j.jdent.2011.03.006>
- Rechmann P, Rechmann BMT, Groves WH, et al. Caries inhibition with a CO<sub>2</sub> 9.3  $\mu\text{m}$  laser: an in vitro study. *Lasers Surg Med* 2016;48(5):546–554. <https://doi.org/10.1002/lsm.22497>
- Rechmann P, Le CQ, Kinsel R, Kerbage C, Rechmann BMT. In vitro CO<sub>2</sub> 9.3- $\mu\text{m}$  short-pulsed laser caries

- prevention—Effects of a newly developed laser irradiation pattern. *Lasers Med Sci* 2020;35(4):979–989. <https://doi.org/10.1007/s10103-019-02940-z>
25. Zuerlein M, Fried D, Featherstone JDB. Modeling the modification depth of carbon dioxide laser treated enamel. *Lasers Surg Med* 1999;25(4):335–347.
  26. Argenta RMO, Tabchoury CPM, Cury JA. A modified pH-cycling model to evaluate fluoride effect on enamel demineralization. *Pesqui Odontol Bras* 2003;17(3):241–246. <https://doi.org/10.1590/S1517-74912003000300008>
  27. Stookey GK, Featherstone JDB, Rapozo-Hilo M, et al. The featherstone laboratory pH cycling model: A prospective, multi-site validation exercise. *Am J Dent* 2011;24(5):322–328.
  28. Featherstone JD, ten Cate JM, Shariati M, Arends J. Comparison of artificial caries-like lesions by quantitative microradiography and microhardness profiles. *Caries Res* 1983;17(5):385–391. <https://doi.org/10.1159/000260692>
  29. Ertuğrul CÇ, Ertuğrul IF. Temperature change in pulp chamber of primary teeth during curing of coloured compomers: An in vitro study using pulpal blood micro-circulation model. *PeerJ* 2019;7:e7284. <https://doi.org/10.7717/peerj.7284>
  30. Krmeek SJ, Miletic I, Simeon P, Mehičić GP, Anić I, Radišić B. The temperature changes in the pulp chamber during cavity preparation with the Er:YAG laser using a very short pulse. *Photomed Laser Surg* 2009;27(2):351–355. <https://doi.org/10.1089/pho.2008.2247>
  31. Cohen JT. The width, the enamel surface area, and the volume of the crown of the deciduous and the permanent teeth. *Int J Orthod Dent Child* 1935;21(5):477–482. [https://doi.org/10.1016/S0097-0522\(35\)90185-X](https://doi.org/10.1016/S0097-0522(35)90185-X)
  32. Zach L, Cohen G. Pulp response to externally applied heat. *Oral Surg Oral Med Oral Pathol* 1965;19(4):515–530. [https://doi.org/10.1016/0030-4220\(65\)90015-0](https://doi.org/10.1016/0030-4220(65)90015-0)
  33. Baldissara P, Catapano S, Scotti R. Clinical and histological evaluation of thermal injury thresholds in human teeth: A preliminary study. *J Oral Rehabil* 1997;24(11):791–801. <https://doi.org/10.1046/j.1365-2842.1997.00566.x>
  34. Dewey WC. Arrhenius relationships from the molecule and cell to the clinic. *Int J Hyperth* 2009;25(1):3–20. <https://doi.org/10.1080/02656730902747919>
  35. Featherstone JD, Nelson DG. Laser effects on dental hard tissues. *Adv Dent Res* 1987;1(1):21–26. <https://doi.org/10.1177/08959374870010010701>
  36. Kim JW, Lee R, Chan KH, Jew JM, Fried D. Influence of a pulsed CO<sub>2</sub> laser operating at 9.4  $\mu\text{m}$  on the surface morphology, reflectivity, and acid resistance of dental enamel below the threshold for melting. *J Biomed Opt* 2017;22(2):28001. <https://doi.org/10.1117/1.JBO.22.2.028001>
  37. Hsu CYS, Jordan TH, Dederich DN, Wefel JS. Laser-matrix-fluoride effects on enamel demineralization. *J Dent Res* 2001;80(9):1797–1801. <https://doi.org/10.1177/00220345010800090501>
  38. Bahrololoomi Z, Fotuhi Ardakani F, Sorouri M. In vitro comparison of the effects of diode laser and CO<sub>2</sub> laser on topical fluoride uptake in primary teeth. *J Dent (Tehran)* 2015;12(8):585–591.
  39. Tepper SA, Zehnder M, Pajarola GF, Schmidlin PR. Increased fluoride uptake and acid resistance by CO<sub>2</sub> laser-irradiation through topically applied fluoride on human enamel in vitro. *J Dent* 2004;32(8):635–641. <https://doi.org/10.1016/j.jdent.2004.06.010>